PHYSICAL MODELING FOR SPATIAL SOUND SYNTHESIS

Alexander Müller and Rudolf Rabenstein

Telecommunications Laboratory
University Erlangen-Nuremberg
Erlangen, Germany
rabe@LNT.de

ABSTRACT

This contribution combines techniques for sound synthesis and spatial reproduction for a joint synthesis of the sound production and sound propagation properties of virtual string instruments. The generated sound field is reproduced on a massive multichannel loudspeaker system using wave field synthesis techniques. From physical descriptions of string vibrations and sound waves by partial differential equations follows an algorithmic procedure for synthesis-driven wave field reproduction. Its processing steps are derived by mathematical analysis and signal processing principles. Three different building blocks are addressed: The simulation of string vibrations, a model for the radiation pattern of the generated acoustical waves, and the determination of the driving signals for the multichannel loudspeaker array. The proposed method allows the spatial reproduction of synthetic spatial sound without the need for pre-recorded or pre-synthesized source tracks.

1. INTRODUCTION

Sound synthesis and sound reproduction are usually seen as separate processes to be performed independently of each other. This point of view originates from the usual workflow in music production. Typically different voices are recorded as separate tracks and then a mix for reproduction for two-channel stereo or surround sound is created. Recent advances in spatial reproduction have increased the number of loudspeaker channels from a few to several tens and even several hundreds. Besides Ambisonics, wave field synthesis has been established as a physically well-founded method for determining the loudspeaker driving signals of such massive multichannel systems [1, 2]. The mixing process for wave field synthesis is much more involved than e.g. stereo amplitude panning. Some authoring tools exist which follow the same workflow of generating loudspeaker signals from recorded tracks for locally distributed moving sound sources [3, 4, 5].

This contribution goes one step further and combines physical modeling sound synthesis with spatial sound reproduction. It extends the physical model for sound synthesis by a model for sound radiation. In this way, not only the wave form of a musical sound but also its spatial characteristics are generated from physical models. They provide the information to calculate the loudspeaker signals for a multichannel reproduction system.

This process is shown here for a specific combination of physical models for sound synthesis, propagation, and reproduction. For physical modeling sound synthesis, a string model with the functional transformation method [6, 7] has been chosen. A simple model for sound propagation is the piston model frequently used as radiation model for loudspeakers [8, 9]. Finally, wave field synthesis is used for spatial sound reproduction.

2. SYSTEM OVERVIEW

A generic model for the sound propagation from a virtual source to a loudspeaker array is shown in Fig. 1. Its basic components are the sound source, its characteristic sound radiation pattern, and a loudspeaker array for reproduction within the listening area. These components are mapped to different building blocks of the joint synthesis and reproduction system as shown in Fig. 2.

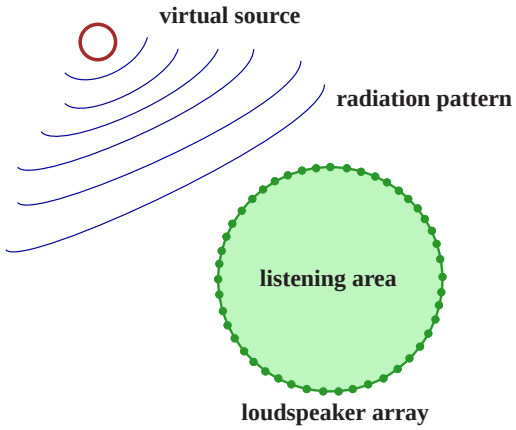

Figure 1: Generic sound propagation model from a virtual source to a loudspeaker array.

The virtual source is realized here by physical modeling sound synthesis for a vibrating string according to the functional transformation method. The user input may consist of a stream of MIDI events which trigger the synthesis algorithm by a short sequence of digital samples as excitation signal. Also the physical properties of the string can be varied by the user at any time.

When the string is attached to a sound board, a part of its energy is radiated into the environment. A piston model is chosen as a simple model for a sound board. This model is closer to the properties of a real sound board than the point source or plane wave models usually employed in wave field synthesis. Furthermore, the piston model is well established in acoustics as a simple loudspeaker model. The position of the piston and its orientation in space may be controlled by the user.

For reproduction of the sound board radiation with an array of loudspeakers, the particle velocity at the location of each loudspeaker has to be known. It can be obtained from the known radiation properties of the piston model. Then the usual techniques for wavefield synthesis reproduction are applied to compute the driving signal for each loudspeaker [2, 10, 11].

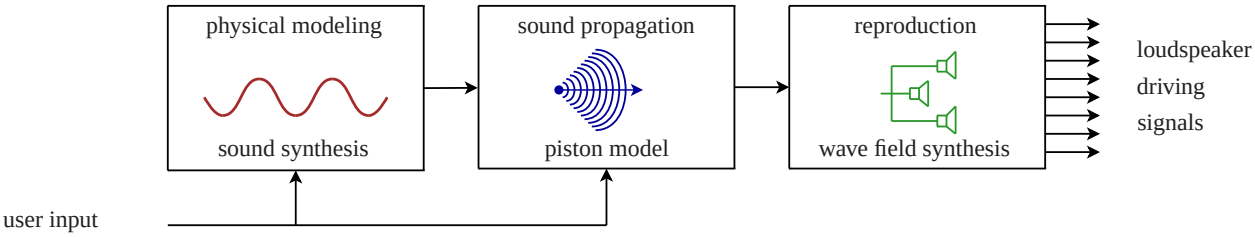

Figure 2: System overview of the combined sound synthesis and wavefield synthesis system.

3. SOUND SYNTHESIS

Physical modeling sound synthesis methods are known to faithfully reproduce the sounds of a variety of timbral classes, like string, drum, bell, pipe sounds and alike. Unlike wavetable synthesis physical modeling offers parametric control of the synthesized sound within its timbral class. Physical modeling methods include digital waveguides [12, 13, 14], mass-spring models [15], component-based models [16] and the functional transformation method [6, 7].

The sound synthesis method in the first block of Fig. 2 is based on a physical model of a vibrating string in the form of a partial differential equation (see e.g. [17, 18])

$$\rho A \frac{\partial^2 y(x,t)}{\partial t^2} + EI \frac{\partial^4 y(x,t)}{\partial x^4} - T_\mathrm{s} \frac{\partial^2 y(x,t)}{\partial x^2} + \\ + d_1 \frac{\partial y(x,t)}{\partial t} + d_3 \frac{\partial^3 y(x,t)}{\partial t \partial x^2} = f_\mathrm{e}(x,t). \quad (1)$$

The independent variable x is the space coordinate along the string with length l ($0 < x < l$) and t is the time coordinate. The dependent variable y denotes the deflection of the string. The excitation is given by the function $f_\mathrm{e}(x,t)$. Table 1 lists the physical parameters.

ρ	density
A	cross section area
E	Young's modulus
I	moment of inertia
T_s	tension of the string
d_1	frequency independent damping
d_3	frequency dependent damping

Table 1: Physical parameters of the string model from (1)

The continuous variable model (1) is turned into a sound synthesis algorithm for the string velocity by the functional transformation method. It has been described in detail e.g. in [6, 7] so that only the block diagram of the resulting algorithm is shown in Fig. 3.

The coefficients $b(\nu)$, $c_0(\nu)$, $c_1(\nu)$, and a_ν for $\nu = 1, \ldots, n$ are calculated directly from the parameters in Table 1. This digital filter structure is excited by a pulse of digital samples $f(k)$ which is triggered e.g. from each MIDI event "note on". The output $v(k)$ closely represents the velocity of the string. The number n of second order sections should be chosen such that all relevant harmonics throughout the audio frequency range are synthesized. In principle, the same algorithm is also suitable for the synthesis of other timbral classes [19].

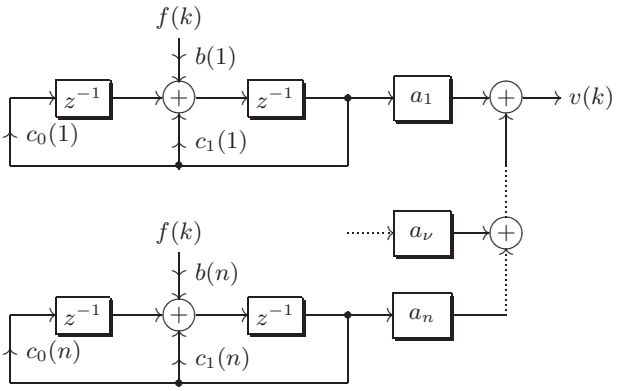

Figure 3: Synthesis algorithm as parallel arrangement of second order digital filters. The blocks labeled z^{-1} are delays by one sample.

4. PISTON MODEL

Strings by themselves do not radiate enough sound energy for the performance of musical sounds. In all acoustical instruments the strings are attached to some kind of sound board. To model this effect, the output of the synthesis algorithms, i.e. the velocity $v(k)$ in Fig. 3, is connected to a piston model.

The piston is a classical model for a loudspeaker with a stiff membrane. Here, it is used as a first approximation to the sound radiation by the sound board of an acoustical instrument. The direct connection between string and sound board is only the most simple model which could be improved by a suitable impedance. More exact models of the radiation of guitars, violines, etc. may require more elaborate models. For example a sound board model consisting of a few discrete piston-oscillators covering the most important resonance peaks has been presented in [20].

The following simple piston model describes the block labeled sound propagation in Fig. 2. Sec. 4.1 presents an analysis of the piston model. Since the resulting integral expression is not easy to evaluate, a classical approximation with a Bessel function is shown in Sec. 4.2. For more details on the piston model, see e.g. [8, 9].

4.1. Analysis of the Piston Model

Fig. 4 shows the coupling between the vibrating string and the piston in all three views of a Cartesian coordinate system with $\mathbf{x} = [x,\ y,\ z]^\mathrm{T}$. The velocity of the string is picked up at an arbitrary position x_a and transfered to the piston (top left for $x_\mathrm{a} = 0$). This kind of coupling may resemble a mechanical connection be-

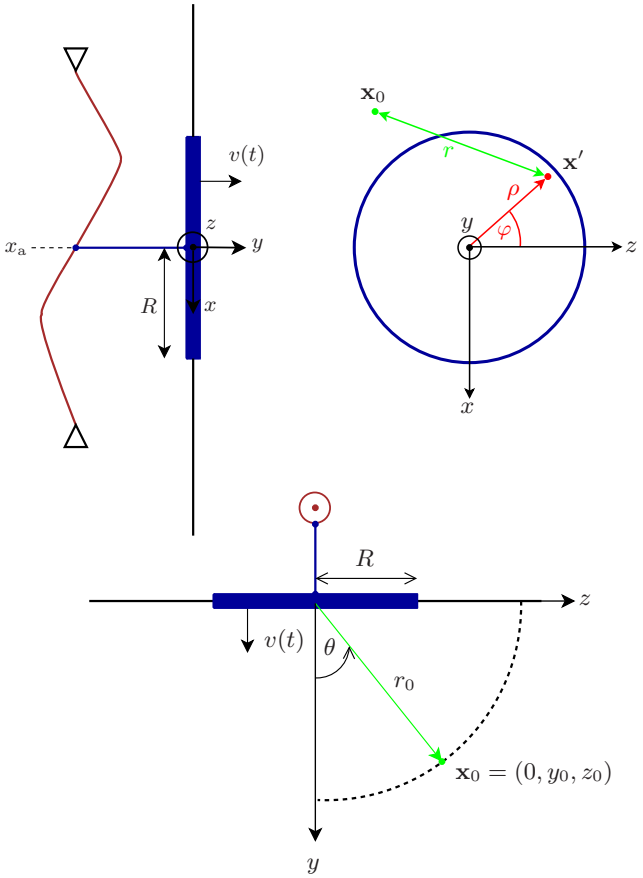

Figure 4: Coupling between the string and the piston,
Top left: view on the x-y-plane,
Top right: Front view of the piston (x-z-plane) with polar coordinates (ρ, φ),
Bottom: view on the y-z-plane; also the point $\mathbf{x}_0$ is here restricted to this plane ($x_0 = 0$).

tween string and soundboard via a bridge or an electrical connection via a magnetic pick-up, an amplifier and a loudspeaker.

The piston can be regarded as a circular disk with radius R located in the x-z-plane which vibrates in the direction of the y-coordinate. The disk is stiff such that all points on the disk have the same phase. Each of these points is modelled as a point source. The sound pressure at an arbitrary point $\mathbf{x}_0$ in the half space with $y > 0$ results from the superposition of the effect of all point sources on the disk. The value of the sound pressure is obtained by integrating over the surface of the disk. The resulting integral relation is most easily expressed in the temporal frequency domain of the continuous time variable t. The velocity $v(t)$ is thus represented by its Fourier transform $V(\omega) = \mathcal{F}\{v(t)\}$. Note that the output of the discrete-time synthesis algorithm from Fig. 3 at a suitable audio sampling rate closely resembles the correct continuous-time velocity $v(t)$.

Now consider the sound pressure $p(t, R, \mathbf{x}_0)$ at the arbitrary location $\mathbf{x}_0$ and its Fourier transform $P(\omega, R, \mathbf{x}_0)$. It can be expressed by the velocity $V(\omega)$ of the piston with radius R through integration over all point sources on its surface A_0

$$P(\omega, \mathbf{x}_0) = j\omega\rho_{\mathrm{L}} V(\omega) \int_{A_0} G(\omega, |\mathbf{x}_0 - \mathbf{x}'|)\, \mathrm{d}A\,. \qquad (2)$$

Here $G(\omega, |\mathbf{x}_0 - \mathbf{x}'|)$ is the free-field Green's function of a point source on the piston at $\mathbf{x}'$ which radiates to a point $\mathbf{x}_0$

$$G(\omega, r) = \frac{e^{-j\omega r/c}}{2\pi r}, \qquad r = |\mathbf{x}_0 - \mathbf{x}'| \qquad (3)$$

The length r denotes the distance between the location $\mathbf{x}_0$ and the variable location $\mathbf{x}'$ on the piston. The corresponding differential surface element on the piston is given by $\mathrm{d}A$. The density of the air is ρ_{L} and the speed of sound is c.

The evaluation of the integral (2) can be found e.g. in [9] and is only briefly presented here. The sound pressure $P(\omega, \mathbf{x}_0)$ is obtained by expressing the coordinates of each point source on the disc by polar coordinates (ρ, φ) as shown on the right of Fig. 4. The components of the Cartesian coordinates of $\mathbf{x}'$ become

$$x' = -\rho \sin\varphi, \quad z' = \rho\cos\varphi, \quad y' = 0, \quad \rho = \sqrt{x'^2 + z'^2}. \qquad (4)$$

The distance

$$r = |\mathbf{x}_0 - \mathbf{x}'| = \sqrt{(x_0 - x')^2 + y_0^2 + (z_0 - z')^2}$$

can be expressed in polar coordinates as

$$r = r(\rho, \varphi) = \sqrt{\rho^2 + 2\rho(x_0 \sin\varphi - z_0 \cos\varphi) + r_0^2} \qquad (5)$$

with

$$r_0^2 = |\mathbf{x}_0|^2 = x_0^2 + y_0^2 + z_0^2\,. \qquad (6)$$

The integral expression in (2) turns with $\mathrm{d}A = \rho\, \mathrm{d}\varphi\, \mathrm{d}\rho$ into

$$P(\omega, R, \mathbf{x}_0) = \frac{j\omega\rho_{\mathrm{L}} V(\omega)}{2\pi} \int_{\rho=0}^{R} \int_{\varphi=0}^{2\pi} \frac{e^{-j\omega r(\rho,\varphi)/c}}{r(\rho, \varphi)} \rho\, \mathrm{d}\varphi\, \mathrm{d}\rho. \qquad (7)$$

Since there is no closed form solution of this integral it has to be evaluated numerically. A simpler representation can only be obtained through certain approximations as is shown next.

4.2. Simplified Piston Model

For an easier evaluation and manipulation of the radiation model, a simplified piston model is preferable. To this end a classical approximation from e.g. [8, 9] is used. It is briefly presented here.

The simplified model is obtained by two different approximations for the term $r(\rho, \varphi)$ in the magnitude and the phase of the Greens's function (3). In the magnitude, r from (3) is approximated by r_0 from (6). This means that the distance of the point at $\mathbf{x}_0$ from the origin replaces the true distance of $\mathbf{x}_0$ to each point source on the piston. This approximation is justified for points $\mathbf{x}_0$ far away from the piston, i.e. $r_0 \gg R \geq \rho > 0$.

Applying the same approximation also to the phase would simply replace the piston by a point source. A better approximation can be obtained for points $\mathbf{x}_0$ that lie in the y-z-plane i.e. $\mathbf{x}_0 = [0,\, y_0,\, z_0]^{\mathrm{T}}$. Alternatively, $\mathbf{x}_0$ can now also be described

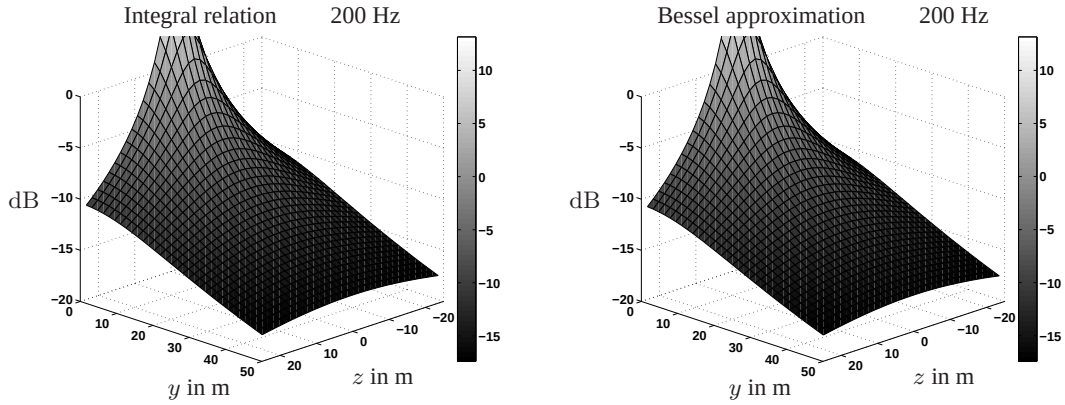

Figure 5: Magnitude response of the piston model for a frequency of 200 Hz. *Left:* Numerical evaluation of the exact integral relation (7)). *Right:* Bessel approximation (12).

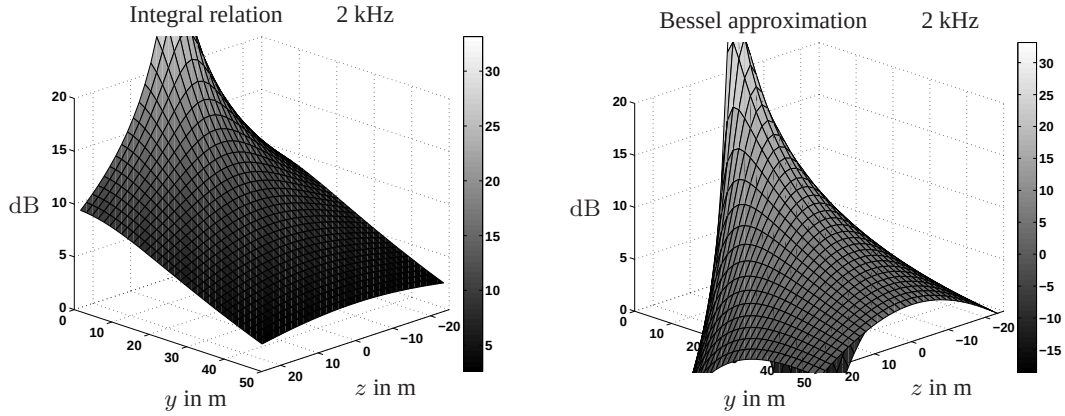

Figure 6: Magnitude response of the piston model for a frequency of 2 kHz. *Left:* Numerical evaluation of the exact integral relation (7)). *Right:* Bessel approximation (12).

by the polar coordinate pair (r_0, θ), where the angle θ is defined on the bottom of Fig. 4.

Considering the radiation of the piston to points in the y-z-plane only is sufficent for modeling the case where sound sources and the reproduction array lie in the same plane.

With $x_0 = 0$, $r_0 \gg \rho$, and a truncated series expansion of the square root, (5) turns into

$$r(\rho, \varphi) = \sqrt{r_0^2 - 2\rho z_0 \cos\varphi} = r_0 - \rho \frac{z_0}{r_0} \cos\varphi \,, \tag{8}$$

or with $z_0 = r_0 \sin\theta$ (see Fig. 4, bottom)

$$r(\rho, \varphi) = r_0 - \rho \sin\theta \, \cos\varphi \,. \tag{9}$$

This relation constitutes the approximation for r in the exponential term in (7).

Inserting the magnitude approximation $r(\rho, \varphi) \approx r_0$ and the phase approximation (9) into the inner integral in (7) gives

$$\begin{aligned} \int_0^{2\pi} \frac{e^{-j\omega r(\rho,\varphi)/c}}{r(\rho,\varphi)} \rho \, \mathrm{d}\varphi &= \frac{\rho}{r_0} e^{-j\omega\tau_0} \int_0^{2\pi} e^{-j\omega\rho \sin\theta \, \cos\varphi \, /c} \, \mathrm{d}\varphi \\ &= \frac{\rho}{r_0} e^{-j\omega\tau_0} \, 2\pi J_0(\omega\rho \sin\theta \, /c) \end{aligned} \tag{10}$$

where J_0 is the Bessel function of the first kind and order zero and

$$\tau_0 = \frac{r_0}{c} = \frac{1}{c}\sqrt{y_0^2 + z_0^2} \,. \tag{11}$$

Performing the outer integration in (7) results finally in (see [9])

$$\tilde{P}(\omega, R, \mathbf{x}_0) = j\omega\rho_\mathrm{L} R^2 \, \frac{J_1(\omega\tau_\theta)}{\omega\tau_\theta} \, \frac{1}{r_0} e^{-j\omega\tau_0} \, V(\omega), \tag{12}$$

where the notation $\tilde{P}$ distinguishes this approximation from the exact relation in (7) and

$$\tau_\theta = \frac{R}{c} \sin\theta = \frac{R}{c} \frac{z_0}{\sqrt{y_0^2 + z_0^2}} \,. \tag{13}$$

The fractional term in (12) involving the Bessel function of the first kind and order zero J_1 behaves similarly to the sinc-function. It is continuous around $\omega = 0$ with

$$\lim_{\omega \to 0} \frac{J_1(\omega\tau_\theta)}{\omega\tau_\theta} = \frac{1}{2}. \tag{14}$$

Equations (11–13) consitute an approximation of the piston's sound pressure field in the y-z-plane. For any point (y_0, z_0), the

relation (12) can be evaluated directly when numerical routines for exponential and Bessel functions are available.

The exact integral relation (7) and the approximation from (11–13) are compared in Figs. 5 and 6. Fig. 5 shows the magnitude of $P(\omega, R, \mathbf{x}_0)$ and $\tilde{P}(\omega, R, \mathbf{x}_0)$ for a selected range of the y-z-plane and a frequency of 200 Hz. Obviously the approximation is quite good. This is also the case for a frequency of 2 kHz (Fig. 6) and for locations normal to the piston, i.e. small values of θ. For larger values of θ, differences in the approximation are visible.

4.3. Sound Pressure Gradient

For loudspeaker reproduction not only the sound pressure but also its gradient are required. It is considered here for the spatially two-dimensional simplified model from Sec. 4.2.

Derivation of $\tilde{P}(\omega, R, \mathbf{x}_0)$ from (12) with respect to the Cartesian coordinates y_0 and z_0 gives

$$\nabla \tilde{P}(\omega, R, \mathbf{x}_0) = \rho_\mathrm{L} c R \, e^{-j\omega\tau_0} \, V(\omega) \begin{bmatrix} A_\mathrm{R} + jA_\mathrm{I} \\ B_\mathrm{R} + jB_\mathrm{I} \end{bmatrix} \quad (15)$$

with

$$A_\mathrm{R} = \frac{y_0}{c r_0 z_0} \, \omega J_1(\omega\tau_\theta) \quad (16)$$

$$A_\mathrm{I} = -\frac{R y_0}{c r_0^3} \, \omega J_1'(\omega\tau_\theta) \quad (17)$$

$$B_\mathrm{R} = \frac{1}{c r_0} \, \omega J_1(\omega\tau_\theta) \quad (18)$$

$$B_\mathrm{I} = -\frac{1}{z_0^2} \, J_1(\omega\tau_\theta) - \frac{R(z_0^2 - r_0^2)}{c z_0 r_0^3} \, \omega J_1'(\omega\tau_\theta). \quad (19)$$

Equations (15–19) allow to calculate the gradient of the sound pressure at any point in the y-z-plane. They provide a reasonable approximation for all locations $\mathbf{x}_0$ with a sufficiently large distance from the piston within the limits shown in Figs. 5 and 6.

5. WAVE FIELD SYNTHESIS

This section presents the combination of the source model introduced above with a wave field synthesis system. At first the geometrical arrangement of source and loudspeaker array is presented. Then the required coordinate transformations are discussed and finally it is shown how to obtain the driving functions for each loudspeaker in the array.

5.1. Geometrical Arrangement

Fig. 7 shows the geometrical arrangement of the virtual sound source – represented by the piston model – and the loudspeaker array for reproduction. The loudspeakers are arranged as a planar array in the plane which contains the vector normal to the piston. Fig. 7 shows a circular array, but also other planar array configurations are possible.

So far, the center of the piston has been considered as the origin of the coordinate system. Now the focus is shifted to the loudspeaker array. Therefore an additional coordinate system is introduced with its origin in the center of the array. For convenience, this new coordinate system is designated with x, y, and z. The coordinates of the piston are now called η and ζ (y and z in the previous section).

In this new coordinate system, the x-y-plane of the array coordinates coincides with the η-ζ-plane of the piston. The origin of the piston coordinate system $(\eta, \zeta) = (0, 0)$ is denoted by $(x, y) = (x_\mathrm{S}, y_\mathrm{S})$. Since piston and array lie in the same plane, the third coordinate can be omitted and only a two-dimensional geometrical arrangement is considered from now on.

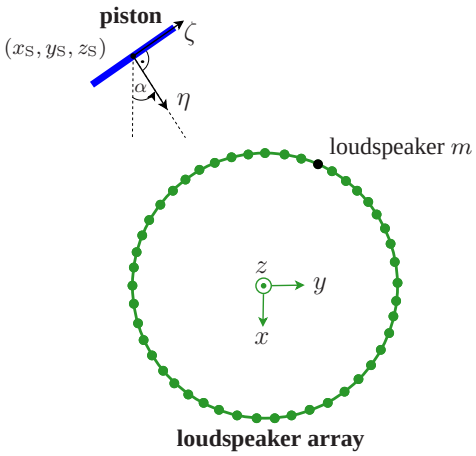

Figure 7: Relation between the coordinate systems of the piston and of the loudspeaker array.

5.2. Coordinate Transformations

For an exact representation of the gradient from (15) in the coordinates of the array, a precise formulation of the transformation between both coordinate systems is required.

The transformation from the piston coordinates (η, ζ) to the array coordinates (x, y) is given by (20) and (21). It includes a rotation by an angle α to align the coordinates and a translation to match the centers of both coordinate systems

$$\begin{bmatrix} x \\ y \end{bmatrix} = \mathbf{R}(\alpha) \begin{bmatrix} \eta \\ \zeta \end{bmatrix} + \begin{bmatrix} x_\mathrm{S} \\ y_\mathrm{S} \end{bmatrix}, \quad (20)$$

$$\mathbf{R}(\alpha) = \begin{bmatrix} \cos\alpha & -\sin\alpha \\ \sin\alpha & \cos\alpha \end{bmatrix}. \quad (21)$$

The inverse transformation from the array coordinates to the piston coordinates is described by (22), where the inverse of the rotation is a rotation by the negative angle

$$\begin{bmatrix} \eta \\ \zeta \end{bmatrix} = \mathbf{R}(-\alpha) \begin{bmatrix} x - x_\mathrm{S} \\ y - y_\mathrm{S} \end{bmatrix}. \quad (22)$$

These coordinate transformations are now used to determine the gradient of the sound pressure at the position of the loudspeakers of the reproduction array. To this end, a certain louspeaker with number m and array coordinates (x_m, y_m) is considered, as shown in Fig. 7. The numerical procedure to obtain the gradient of the piston's sound pressure at the location (x_m, y_m) is shown in Fig. 8.

It consists of the following steps:

- transform the array coordinates (x_m, y_m) of loudspeaker m into the piston coordinates (η_m, ζ_m) using (22),

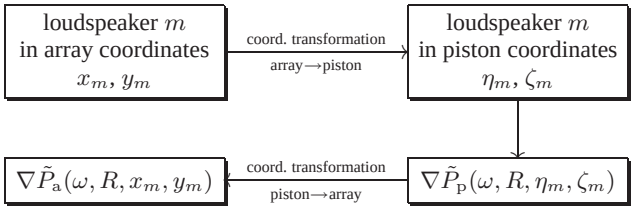

Figure 8: Coordinate transformations to obtain the gradient of the sound pressure for loudspeaker number m from the piston model.

- compute the gradient of the sound pressure from (15). The location of the loudspeaker (η_m, ζ_m) in piston coordinates is used here for the arbitrary location $\mathbf{x}_0$ in (15). The subscript p indicates that the gradient is represented in piston coordinates.
- use (20) to transform the gradient $\tilde{P}_\mathrm{p}$ from piston coordinates into the corresponding expression $\tilde{P}_\mathrm{a}$ for the gradient of the sound pressure in array coordinates (x_m, y_m).

This numerical procedure provides the gradient of the piston's sound pressure at all positions of the loudspeaker array.

5.3. Loudspeaker Driving Functions

In a last step the driving functions for each loudspeaker of the reproduction array have to be determined. According to [11], these driving functions are obtained from the gradient of the sound pressure at the loudspeaker position by application of

- a spatial window $w(\mathbf{x}_m, \mathbf{x}_\mathrm{S})$ which selects the active loudspeakers for a certain source direction,
- an amplitude factor $A(\mathbf{x}_m)$ which depends on the position $\mathbf{x}_m$ of the loudspeaker with number m,
- a frequency selective filter $H_\mathrm{wfs}(\omega)$ which is independent of the loudspeaker position

$$D(\omega, \mathbf{x}_m) = w(\mathbf{x}_m, \mathbf{x}_\mathrm{S}) A(\mathbf{x}_m) H_\mathrm{wfs}(\omega) \frac{\partial}{\partial \mathbf{n}} P(\omega, \mathbf{x}_m). \quad (23)$$

The vector $\mathbf{x}_m$ denotes the location (x_m, y_m) of loudspeaker m in the x-y-plane. Similarly, $\mathbf{x}_\mathrm{S}$ is the position $(x_\mathrm{S}, y_\mathrm{S})$ of the piston.

The spatial window function $w(\mathbf{x}_m, \mathbf{x}_\mathrm{S})$ selects those loudspeakers that are active for the reproduction of a certain virtual source. It depends on the direction of two vectors: The vector indicating the direction from the source at $\mathbf{x}_\mathrm{S}$ to the loudspeaker at $\mathbf{x}_m$ and the normal vector $\mathbf{n}_m$ on the surface of the loudspeaker array. For the loudspeaker arrangement of Fig. 7 this vector points inwards from the loudspeaker m towards the center of the circular array, i.e. the origin of the array coordinate system. The window function is positive if the scalar product of these vectors is positive and zero otherwise.

The amplitude factor $A(\mathbf{x}_m)$ and the transfer function $H_\mathrm{wfs}(\omega)$ result from the fact that a three-dimensional wave field is reproduced with a planar array (see [11, chapter 13.2]).

The normal derivative of $P_\mathrm{a}(\omega, \mathbf{x}_m)$ at the louspeaker position $\mathbf{x}_m$ in (23) can be expressed by the transpose of the above normal vector $\mathbf{n}_m$ and the gradient of the sound pressure from (15) as

$$\frac{\partial}{\partial \mathbf{n}} P(\omega, \mathbf{x}_m) = \mathbf{n}_m^\mathrm{T} \, \nabla \tilde{P}_\mathrm{a}(\omega, R, \mathbf{x}_0). \quad (24)$$

Combining (15), (23) and (24) gives

$$D(\omega, \mathbf{x}_m) = H_\mathrm{rad}(\omega, \mathbf{x}_m) A(\mathbf{x}_m) H_\mathrm{wfs}(\omega) V(\omega) \quad (25)$$

with

$$H_\mathrm{rad}(\omega, \mathbf{x}_m) = w(\mathbf{x}_m, \mathbf{x}_\mathrm{S}) \rho_\mathrm{L} c R \, e^{-j\omega\tau_0} \, \mathbf{n}_m^\mathrm{T} \begin{bmatrix} A_\mathrm{R} + jA_\mathrm{I} \\ B_\mathrm{R} + jB_\mathrm{I} \end{bmatrix}. \quad (26)$$

The time constant τ_0 from (11) and the vector components from (16-19) have to be computed with the coordinate transformations from Sec. 5.2.

Eq. (25) gives the (Fourier transform of the) loudspeaker driving signal for loudspeaker m. It uses the string velocity $V(\omega)$ from the physical modeling sound synthesis algorithm from Sec. 3 as input and computes the driving signal by filtering operations. The transfer function $H_\mathrm{rad}(\omega, \mathbf{x}_m)$ results from the radiation model presented in Sec. 4.2 applied to each active loudspeaker. The gain factor $A(\mathbf{x}_m)$ and the transfer function H_wfs have been introduced above.

6. SIGNAL PROCESSING STRUCTURE

This section presents a signal processing structure which realizes the simplified piston model from Sec. 4.2. Further approximations for more efficient processing are shortly discussed.

6.1. Signal Processing Structure for the Piston Model

The determination of the loudspeaker driving functions according to (25) closely resembles the block diagram from Fig. 2:

1. The string velocity is the result of the sound synthesis in the first block. The structure of the corresponding synthesis algorithm through the functional transformation method has been shown in Fig. 3 from Sec. 3.
2. The sound propagation model in the second block is given by the transfer functions $H_\mathrm{rad}(\omega, \mathbf{x}_m)$ for each loudspeaker m. They are based on the simplified piston model according to Sec. 4.2.
3. The third block is realized by the gain factor $A(\mathbf{x}_m)$ and the transfer function $H_\mathrm{wfs}(\omega)$ as described in Sec. 5.

Fig. 9 shows a more detailed version of Fig. 2 with the transfer functions and factors listed above. It represents the signal processing structure for computing the driving functions of a wave field synthesis system as triggered by musical events from a MIDI source or other kind of human input.

The structure of Fig. 9 follows closely the decomposition into functional blocks from Fig. 2 and even Fig. 1. However, it appears that the realization of the blocks from Fig. 2 according to Fig. 9 is not the most efficient one. Each branch for the individual loudspeakers contains the transfer function $H_\mathrm{wfs}(\omega)$ which is independent of the loudspeaker position and thus the same for all branches. A first attempt would be to shift $H_\mathrm{wfs}(\omega)$ to the output of the sound synthesis model such that this filtering operation has to be performed only once. A more efficient processing structure can be obtained with further approximations.

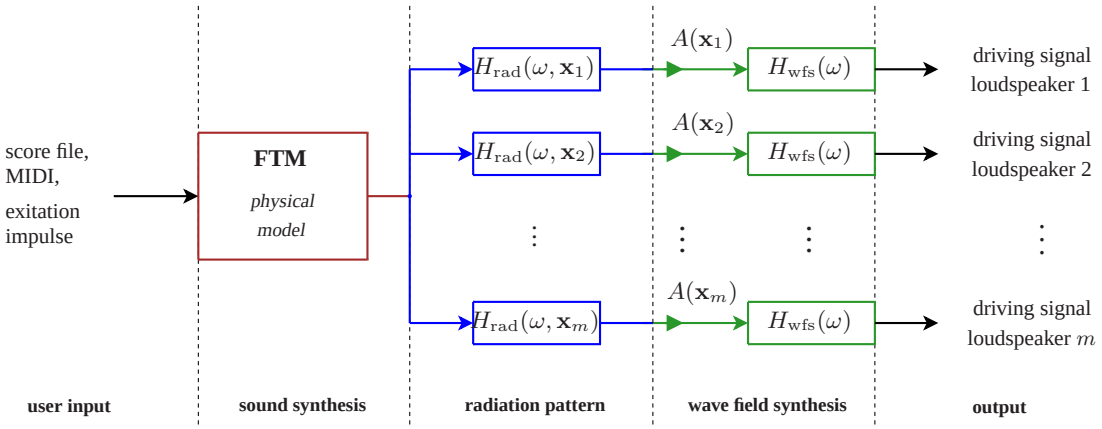

Figure 9: Signal processing structure from MIDI input to loudspeaker outputs.

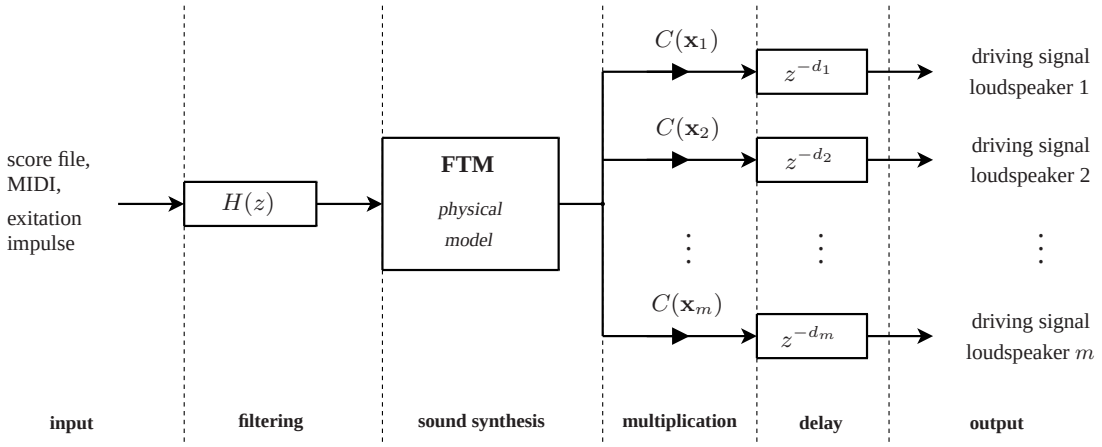

Figure 10: Efficient implementation of the discrete-time signal processing structure by combination of transfer functions and amplitude factors across the block boundaries.

6.2. Simplified Signal Processing Structure

A more efficient structure for the determination of the driving signals can be obtained by further approximations. Rather than only using geometrical approximations as in Sec. 4.2, techniques from the design of digital filters may be applied to approximate the transfer function $H_{\mathrm{rad}}(\omega, \mathbf{x}_m)$ from (26) by a simpler transfer function of the general form

$$H_{\mathrm{rad}}(\omega, \mathbf{x}_m) \approx \tilde{H}_{\mathrm{rad}}(\omega) B(\mathbf{x}_m) e^{-j\omega\tau_m}. \qquad (27)$$

Here the transfer function $\tilde{H}_{\mathrm{rad}}(\omega)$ is the same for all loudspeakers, while the gain factor $B(\mathbf{x}_m)$ and the phase term $e^{-j\omega\tau_m}$ vary for each loudspeaker position m. The methods to choose $\tilde{H}_{\mathrm{rad}}(\omega)$, $B(\mathbf{x}_m)$, and τ_m for a good approximation of $H_{\mathrm{rad}}(\omega, \mathbf{x}_m)$ in a certain sense are not discussed here.

Instead the signal processing structure which results from this simplification is shown in Fig. 10. Due the simple form of (27), all filtering operations are independent of the loudspeaker position. Therefore the transfer functions $H_{\mathrm{wfs}}(\omega)$ from Fig. 9 and $\tilde{H}_{\mathrm{rad}}(\omega)$ from (27) can be combined into one discrete-time transfer function $H(z)$ shown in Fig. 10. A Fourier-type approximation of the continuous-time transfer functions has been applied, which results in a realization of $H(z)$ by an FIR filter of order up to 256.

Since the sound synthesis algorithm by the functional transformation method (FTM) is a linear system, the filtering operation by $H(z)$ and the synthesis algorithm may be interchanged. As shown in Fig. 10, the output of $H(z)$ is the input signal for the sound synthesis block. It is thus not required to perform a filtering operation with $H(z)$. Instead each MIDI note event triggers the pre-stored impulse response of $H(z)$ to feed the sound synthesis algorithm. The same principle has been used for a so-called commuted piano synthesis in [21].

The simple radiation model from (27) and the driving functions contain also amplitude factors for each loudspeaker position which can be combined into one factor each ($C(\mathbf{x}_m)$ in Fig. 10). Finally there remain only the delays from the simple radiation model which are specific for each loudspeaker. The delays d_m in samples result from the time constants τ_m in seconds via the sample rate.

Comparing the structures in Fig. 9 and Fig. 10 shows that now the branches for each loudspeaker are free from any filtering operations. Since the number of loudspeakers is in the order of tens

or hundreds, the resulting signal processing structure shown in Fig. 10 allows for a more efficient realization. The quality of the spatial reproduction depends on the quality of the approximation in (27). The trade-off between numerical expense and reproduction quality can only be established by listening tests. In any case, the structure in Fig. 9 provides a physically well found model with a moderate geometrical approximation at the expense of filtering each single loudspeaker channel.

These signal processing structures have been implemented for reproduction with a 48-channel wave field synthesis system at the Telecommunications Laboratory of the University Erlangen-Nürnberg. Musical examples with multiple strings at different locations and with the movement of sources along their individual trajectories demonstrate the feasibility of this joint synthesis and reproduction method. Listening tests with the simplified piston model in various distances show that this model allows for a gradual variation of the sound between its two extremes, a distant point source and a plane wave.

7. CONCLUSIONS

Physical modeling sound synthesis has been confined so far to the production of monophonic or two-channel stereo sound. Its capability for spatial reproduction is greatly enhanced by the combination with wave field synthesis. Both physical modeling sound synthesis and wave field synthesis rely on physical models in the form of partial differential equations. The missing link between a synthesized sound source and its reproduction by wave field synthesis is the spatial radiation pattern of the virtual instrument. The well-known and proven piston model has been used here as a proof of concept. It can be implemented directly by a suitable signal processing structure or it can serve as starting point for further simplifications of the multichannel algorithm. It has been verified by listening tests that the promises of physical modelling hold, i.e. not only the timbre of the sound but also the location, orientation, and motion of the source are subject to parametric control by the user. The appropriateness of the piston model and its simplifications for specific families of instruments like violins, brass instruments, or pianos have still to be established by more detailed modelling and testing.

8. REFERENCES

[1] A.J. Berkhout and D. de Vries, "Acoustic holography for sound control," in *86th AES Convention*. Audio Engineering Society (AES), March 1989, Preprint 2801 (F-3).

[2] Jens Ahrens, Rabenstein Rudolf, and Sascha Spors, "The theory of wave field synthesis revisited," in *124th AES Convention*. Audio Engineering Society, May 2008, Paper number 7358.

[3] Thomas Sporer, "Wave field synthesis – generation and reproduction of natural sound environments," in *Proc. of the 7th Int. Conf. on Digital Audio Effects (DAFx'04)*, Naples, Italy, Oct. 2004, pp. 133–138.

[4] Frank Melchior, Tobias Lauterbach, and Diemer de Vries, "Authoring and user interaction for the production of wave field synthesis content in an augmented reality system," in *Proc. of the Int. Symp. on Mixed and Augmented Reality (ISMAR'05)*, 2005.

[5] S. Bleda, J.J. Lopez, J. Escolano, and B. Pueo, "A flexible authoring tool for wave field synthesis," in *Proc. of Int. Computer Music Conference (ICMC 2005)*, Barcelona, 2005.

[6] L. Trautmann and R. Rabenstein, *Digital Sound Synthesis by Physical Modeling of Musical Instruments using Functional Transformation Models*, Kluwer Academic/Plenum Publishers, Boston, USA, 2003.

[7] R. Rabenstein and L. Trautmann, "Digital sound synthesis of string instruments with the functional transformation method," *Signal Processing*, vol. 83, pp. 1673–1688, 2003.

[8] Leo L. Beranek, *Acoustics*, Acoustical Society of America, 1993.

[9] Manfred Zollner and Eberhard Zwicker, *Elektroakustik*, Springer-Verlag, Berlin, 1993.

[10] R. Rabenstein and S. Spors, "Sound reproduction," in *Springer Handbook of Speech Processing*, J. Benesty, M. Sohndi, and Y. Huang, Eds., chapter 53, pp. 1095–1114. Springer, Berlin, 2008.

[11] R. Rabenstein, S. Spors, and P. Steffen, "Wave field synthesis techniques for spatial sound reproduction," in *Topics in Acoustic Echo and Noise Control*, E. Hänsler and G. Schmidt, Eds., pp. 517–545. Springer, 2006.

[12] Julius. O. Smith III, "Physical modeling synthesis update," *Computer Music J.*, vol. 20, no. 2, pp. 44–56, 1996.

[13] M. Kahrs and K. Brandenburg, Eds., *Applications of Digital Signal Processing to Audio and Acoustics*, Kluwer Academic Publishers, Boston, 1998.

[14] V. Välimäki, J. Pakarinen, C. Erkut, and M. Karjalainen, "Discrete-time modelling of musical instruments," *Rep. Prog. Phys.*, vol. 69, no. 1, pp. 1–78, January 2006.

[15] Alexandros Kontogeorgakopoulos and Claude Cadoz, "Cordis Anima physical modeling and simulation system analysis," in *Proc. SMC'07, 4th Sound and Music Computing Conf.*, Lefkada, Greece, July 2007, pp. 275–281.

[16] Panagiotis Tzevelekos, Thanassis Perperis, Varvara Kyritsi, and Georgios Kouroupetroglou, "A component-based framework for the development of virtual musical instruments based on physical modeling," in *Proc. SMC'07, 4th Sound and Music Computing Conf.*, Lefkada, Greece, 2007, pp. 30–36.

[17] A. Chaigne and A. Askenfelt, "Numerical simulations of piano strings. I.A physical model for a struck string using finite difference methods," *J. Acoust. Soc. Am.*, vol. 95, no. 2, pp. 1112–1118, 1994.

[18] Neville H. Fletcher and Thomas D. Rossing, *The Physics of Musical Instruments*, Springer-Verlag, New York, NY, USA, 2nd edition, 1998.

[19] Stefan Petrausch and Rudolf Rabenstein, "Block-based physical modeling for digital sound synthesis of membranes and plates," in *International Computer Music Conference (ICMC)*, Barcelona, Spain, Sept. 2005.

[20] O. Christensen, "An oscillator model for analysis of guitar sound pressure response," *Acustica*, vol. 54, pp. 289–295, 1984.

[21] J.O. Smith III and S.A. Van Duyne, "Overview of the commuted piano synthesis technique," in *Applications of Signal Processing to Audio and Acoustics, 1995., IEEE ASSP Workshop on*, Oct 1995, pp. 226–229.